

# When the Source of Flooding **Matters: Divergent Responses** in Carbon Fluxes in an Alaskan Rich Fen to Two Types of Inundation

E. S. Euskirchen, <sup>1</sup>\* E. S. Kane, <sup>2,3</sup> C. W. Edgar, <sup>1</sup> and M. R. Turetsky <sup>4</sup>

<sup>1</sup>Institute of Arctic Biology, University of Alaska Fairbanks, 902 N. Koyukuk Dr., Box 757000, Fairbanks, Alaska 99775, USA; <sup>2</sup>School of Forest Resources and Environmental Sciences, Michigan Technological University, Houghton, Michigan 49931, USA; <sup>3</sup>U.S. Forest Service, Northern Research Station, Houghton, Michigan 49931, USA; <sup>4</sup>Department of Integrative Biology, University of Guelph, Guelph, Ontario NIG IG2, Canada

#### ABSTRACT

The extent of groundwater-influenced rich fens is increasing across northern regions as permafrost thaws. The increase in the extent of these fens, which store large amounts of carbon in deep organic deposits, is coupled to increases in rainfall and runoff. We examine interannual variations in carbon and water fluxes at a rich fen in interior Alaska that included early (May–June) and mid-late (July–September) dry and wet periods, with early season wet periods coincident with runoff from snowmelt and later season wet periods coincident with inundation from rainfall. From May 2011 to December 2018, the fen was estimated as a 170  $\pm$  64 g C m<sup>-2</sup> source of CO<sub>2</sub>. When controlling for soil temperature, net CO2 uptake was greatest during the early season under dry conditions,

with the water table position below the surface, and least during the mid-late season when the water table position was above the surface. Methane emissions were lowest during early season wet periods and greatest during late season wet periods. Our results suggest that it is important to consider the seasonality of wet and dry periods, and how these may potentially be related to runoff from snowmelt versus rainfall in boreal rich fens, when considering the annual net C balance and making accurate projections of carbon balance in northern wetlands.

Key words: Boreal; Rainfall; Runoff; Permafrost thaw; Water balance; Net ecosystem exchange; Methane emissions.

#### **HIGHLIGHTS**

• A boreal rich fen in interior Alaska is a source of

- CO<sub>2</sub> and CH<sub>4</sub> from 2011 to 2018.
- Received 28 June 2019; accepted 23 October 2019

Author Contributions ESE, ESK, and MRT designed the study. ESE, ESK, and CWE analyzed data. All authors performed the research. ESE wrote the paper with contributions from all authors.

\*Corresponding author; e-mail: seeuskirchen@alaska.edu

- Characteristics of inundation, including its timing either in spring or mid-late season, influenced the release of C as CO2 versus CH4.
- Warming winter soil temperatures were also related to increases in CO<sub>2</sub> emissions.

#### Introduction

Northern peatlands contain about 20% of the soil organic carbon in the world, approximately  $500 \pm 110$  Gt C (Yu 2012). Boreal rich fens are one

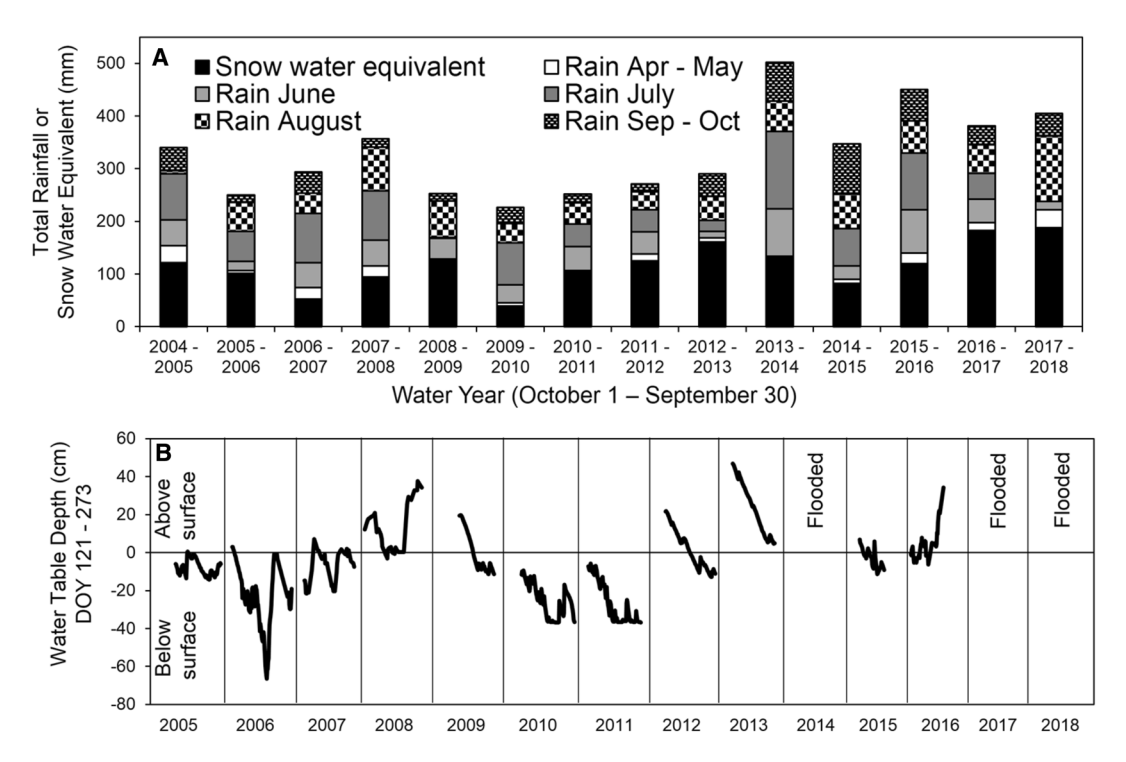


**Figure 1.** In (**a**), total snow water equivalent and rain (mm) for each water year October 1, 2004–September 30, 2018. In **b**, water table depth (cm) from May to September. In years marked as flooded, water table depth exceeded 60 cm above the surface and was not measured.

of the most common peatland types in western boreal North America (Vitt and others 2000), and open peatlands and mineral wetlands comprise about 85% of wetland area in (311,758 km<sup>2</sup>; Kolka and others 2018). With rapid accumulation of both herbaceous and moss-derived peat, they store large amounts of carbon in their deep organic deposits, acting to mitigate climate change. These rich fens are influenced by lateral water movement, or water sources that have been in contact with a nutrient-rich surface or groundwater, making them productive and biologically diverse. The areal extent of these fens in interior Alaska has increased with permafrost degradation and changing ground- and surfacewater relationships. From 1949 to 1995, the area of rich fens in the Tanana Flats of interior Alaska increased from 31 to 40% as permafrost degraded in lowland birch and black spruce forests (Jorgenson and others 2001). Increasing area of fens is expected to continue, particularly as lowland birch forests continue to undergo permafrost degradation (Lara and others 2016). Expansion of fens also is thought to be a key mechanism accelerating permafrost thaw in the discontinuous permafrost zone in Northwest Canada (Helbig and others 2016).

Precipitation, runoff, and groundwater provide water to fens, and these water sources are expected

to change in the future, coupled with the increases in the areal extent of fens. Predicted increases in rainfall in interior Alaska range between 10 and 20 mm per decade from 2009 to 2100 (Euskirchen and others 2016). These decadal increases are also likely to occur with increases in the number of extreme daily rainfall events (Tebaldi and others 2006; Lehmann and Coumou 2015). Snowfall is also expected to increase by approximately 10-20 mm per decade from 2009 to 2100. However, snow return is expected to occur later and snow melt is expected to occur earlier, resulting in a decrease in the length of the period of snow-covered ground in interior Alaska by 5 days per decade from 2009 to 2100 (Euskirchen and others 2016). Moreover, Alaskan fens are found in low-lying areas where hydrology is influenced both by local permafrost degradation and by runoff from upland ecosystems. Fens are susceptible to inundation as permafrost thaws, and the upwelling of melt water increases (Jorgenson and Osterkamp 2005). Thus, interior Alaskan fens will likely become more common and wetter because of increases in both rain and snow, combined with greater groundwater discharge and runoff. The resiliency of these ecosystems to changes in water balance, from a C balance perspective, is still not well understood.

Boreal fens are typically regarded as net sinks of CO<sub>2</sub>. The amount of CO<sub>2</sub> these ecosystems take up has been attributed to a number of factors, including water table depth, timing of snowmelt, pre-growing season air temperature, growing season length, and growing season temperature (Aurela and others 2004, 2009; Flanagan and Syed 2011; Peichl and others 2014; Jammet and others 2017). The gross primary productivity (GPP) of boreal fens is largely dependent on both water table depth and temperature (Sulman and others 2010), although temperature alone may act as the primary explanatory variable up to a threshold water table depth above the surface (Sonnentag and others 2010; but see also Laine and others 2019). Ecosystem respiration (ER) in these fens has also been explained by both temperature and water table depth, with wetter conditions inhibiting ER (Sulman and others 2010), although other work has found that water table depth has little influence on ER (Olefeldt and others 2017).

Boreal fens are also sources of methane (CH<sub>4</sub>), with emissions peaking in July and August, in conjunction with a peak in the vascular plants that mediate CH<sub>4</sub> emissions to the atmosphere (Peichl and others 2014; Jammet and others 2017). Wetter conditions in these fens promote greater CH<sub>4</sub> emissions (Turetsky and others 2008; Olefeldt and others 2017). The inclusion of CH<sub>4</sub> to the annual net CO<sub>2</sub> uptake of a boreal fen may or may not result in a net loss of carbon to atmosphere (Rinne and others 2018; Webster and others 2018).

In May 2011, we initiated eddy covariance measurements of CO<sub>2</sub>, water, and energy fluxes at the Alaska Peatland Experiment (APEX) rich fen in the Tanana Flats of interior Alaska, with eddy covariance of CH<sub>4</sub> beginning in 2014. These measurements augmented chamber measurements of CO2 and CH4 fluxes that began in 2005 in conjunction with a water table manipulation experiment in a subsection of the fen (Turetsky and others 2008; Chivers and others 2009; Olefeldt and others 2017). The analysis of Euskirchen and others (2014) included just 2.5 years of eddy covariance measurements of CO<sub>2</sub> (May 2011–December 2013), and did not include eddy covariance measurements of CH<sub>4</sub>. We have now supplemented these CO<sub>2</sub> measurements through 2018, and also included the eddy covariance measurements of  $CH_4$ , beginning in 2014.

From 2013 to 2018, conditions at the site were wetter than the previous years since measurements began in 2005. The site experienced both early (May–June) and mid-late season (July, August, September) inundation, with early season inun-

dation largely ascribed to high snowfall driving a more pronounced freshet, whereas late season inundation was maintained through high rainfall throughout the summer. We investigated seasonality in terms of early versus later growing season inundation as a driver of ecosystem carbon fluxes. We focused our analysis on the period during which the eddy covariance data were collected, May 2011–December 2018.

#### **Methods**

### Site Description

The rich fen is in the boreal peatland lowlands of the Tanana Flats of interior Alaska (64.70° N, 148.32° W, 100 m elevation), approximately 30 km southeast of Fairbanks. The site is within a floodplain and is approximately 2 km from the Tanana River. While the surrounding landscape contains permafrost, this site lacks near-surface permafrost. The peat depth is 1-2 m. The vegetation is comprised of emergent vascular species (Equisetum, Carex, and Potentialla), small amounts of brown moss and Sphagnum, and no trees (cf. Churchill and others 2015; McPartland and others 2019). Detailed descriptions of the site are provided in Turetsky and others (2008), Chivers and others (2009), Kane and others (2010), and Euskirchen and others (2014). The site is associated with the Bonanza Creek Long Term Ecological Research Program (lter.uaf.edu).

## Measurements

#### Eddy Covariance and Biophysical Measurements

Eddy covariance measurements of CO<sub>2</sub>, latent, and sensible heat and associated meteorological measurements commenced in May of 2011 in an area of the fen that was outside the footprint of both raised and lowered water table treatments (Euskirchen and others 2014). Measurements of the meteorological data have been continuous since May of 2011, but two longer gaps in the eddy covariance data occurred due to either power limitations or instrument failure. These include a gap from November 5, 2011, to December 31, 2011, and a gap from March 6, 2016, to May 4, 2016. In May of 2014, we initiated eddy covariance measurements of CH<sub>4</sub>, with collection occurring from late April or early May through late September or early October each year from 2014 to 2018. Measurements of CH<sub>4</sub> were not collected year-round due to power limitations. Although the setup and data processing of these measurements were previously described in Euskirchen and others (2014), we also describe them briefly here.

Due to the remote location of the site and the absence of line power, electrical power for instrumentation was provided by solar panels and batteries, with the occasional use of a generator during the months of December and January. Initially, the power supply at the fen site consisted of three 12-V absorbent glass mat batteries charged by a single 200-W solar panel, but in 2014, the system was augmented to consist of 1400-W crystalline photovoltaic arrays charging a large ( $\sim$  5000 A h) 12-V absorbent glass mat battery bank. The eddy covariance system for measuring the fluxes of CO<sub>2</sub>, CH<sub>4</sub> water, and energy was mounted in the center of the sites at 2 m height.

The instrumentation consisted of an EC-150 for CO<sub>2</sub>, water and energy fluxes (Campbell Scientific Instruments, Logan, Utah, USA) and a fast-response open-path methane analyzer (LI-7700; LI-COR, Lincoln, Nebraska, USA) which used a LI-7550 interface unit to control mirror heating and cleaning cycles and to route the high-frequency data to the datalogger. All instrumentation was connected to a digital datalogging system to log data at 10 Hz intervals.

Basic microclimatic data were also collected, including photosynthetically active radiation (PAR; 2 m above the ground; LI190SB, LI-COR), air temperature (Ta) and relative humidity (RH; 2 m above the ground; HMP45C, Vaisala, Helsinki, Finland), soil water content (water content reflectometer, CS616, Campbell Scientific Instruments), soil heat flux (G, two replicates at 5 cm below the surface, HFP01-SC, Hukseflux, Delft, Netherlands), precipitation as rain was measured with a tipping bucket (at 2 m above the ground; TE525MM, Texas Electronics, Dallas, Texas, USA), net radiation (Rn; at 2 m above the ground; NR-LITE; Kipp and Zonen, Delft, Netherlands), snow depth (at 2 m above the ground; SR50A, Campbell Scientific Instruments), albedo (at 2 m above the ground; albedometer CMA6, Kipp and Zonen), soil temperature (T<sub>s</sub> at 2 and 6 cm depth; TCAV; averaging soil thermocouple probe; Campbell Scientific Instruments), and barometric pressure (Pa; PB105, Vaisala). Snow water equivalent (SWE) data were collected with a precipitation weighing assembly (ETI NOAH III; Fort Collins, CO, USA; Van Cleve and others 2018). These variables were measured at 1-s intervals and stored in the datalogging systems. Both the processed eddy covariance and microclimatic data were averaged for 30-min periods. Photographic images were collected once a day

with a StarDot Netcam (StarDot Technologies, Buena Park, CA, USA).

Water table levels were measured using a pressure transducer (Campbell Scientific, Logan, Utah) installed at the bottom of a 5-cm-diameter, 1-mlong PVC well. The spatial variability of the water table was determined with weekly manual measurements of water table position within six other permanent wells in the fetch of the flux tower. To examine the effect of early versus mid-late season wet (water table depth > 0 cm) and dry (water table depth  $\leq 0$  cm) periods on carbon fluxes, the inundation status of the fen was classified from May to September of the years 2011-2018 when information pertaining to the water table depths was available. These classes include: (1) early season dry: days in May and June when the water table is below the surface; (2) early season wet/ inundated: days in May and June when the water table is above the surface; (3) mid-late season dry: days in July, August, or September when the water table is below the surface; and (4) mid-late season wet/inundated: days in July, August, or September when the water table is above the surface.

#### Chamber Measurements

The static chamber technique was used to measure CO<sub>2</sub> and CH<sub>4</sub> effluxes from the peat surface as previously described in detail ('control' site described by Turetsky and others 2008 and Chivers and others 2009). Briefly, six collars ( $60 \times 60$  cm) were inserted to a depth of 10 cm in 2005. A clear lexan chamber (0.227 cm<sup>3</sup>) with closed-cell foam sealed the chamber with the collar during measurements. Two computer CPU fans mixed the air within the chamber during measurements. The change in chamber CO2 concentrations was measured for approximately 4 min using a portable infrared gas analyzer (IRGA; PP Systems EGM-4, Amesbury, Massachusetts, USA). Ecosystem respiration was measured by chamber measurements while shaded with an opaque shroud, and net primary production was measured without a shroud. Temperature, relative humidity, and PAR were logged continuously within the chamber during each flux measurement with a PP Systems TRP-1 sensor. CH<sub>4</sub> efflux measurement campaigns were coordinated with CO2 efflux measurements (usually within a day). Chambers were closed for approximately 30 min, and seven 20-mL gas samples were taken over time (time zero, and every 5 min). Syringe gas samples were analyzed within 24 h, using a Varian 3800 gas chromatograph with a FID detector with a Haysep N column (Varian Analytical Inc., Palo Alto, California, USA). In this study, we compared chamber- and eddy covariance-based measurements when data from common measurement periods were available. This included campaigns in June–August in years 2015–2016 for CH<sub>4</sub>, and in years 2011, 2012, 2013, 2015 and 2016 for CO<sub>2</sub>.

# Data Processing and Post-processing

Eddy covariance data processing and post-processing were done as described in Euskirchen and others (2014). A CO<sub>2</sub> signal strength diagnostic, which represents optical impedance by precipitation or aerial contaminants, is provided by the EC-150 IRGA. This diagnostic was used as a quality assurance/quality control variable for both flux and radiation data, with 70% as the minimum EC-150 threshold. The 'WPL' terms were applied during post-processing to the CO<sub>2</sub> and latent heat fluxes to account for changes in mass flow caused by changes in air density (Webb and others 1980). Corrections were applied to account for frequency attenuation of the eddy covariance fluxes (Massman 2000, 2001). To account for nocturnal CO<sub>2</sub> advection, we calculated a storage term and then performed a friction velocity (u\*) correction for calm periods, when  $u^*$  was less than 0.2 m s<sup>-1</sup>.

Data gaps occurred because of instrument malfunction, power outages, or occasional generator use in December and January. Shorter gaps in the eddy covariance data were usually related to instrument errors during precipitation events in the summer and winter. Longer gaps occurred due to power outages and instrument shutdown during cold temperatures. For data gaps in net ecosystem exchange (NEE) and CH<sub>4</sub> of approximately 1-6 days, we gap-filled by calculating the mean diurnal variation, where a missing observation is replaced by the mean for that time period (half hour) based on adjacent days (Falge and others 2001). This method provided stable approximations of missing data using 7-day independent windows during the nighttime hours and 14-day windows during the daytime hours (Falge and others 2001).

We calculated ecosystem respiration (ER) following the methodology described in Euskirchen and others (2017). Net ecosystem exchange (NEE) is the difference between gross  $CO_2$  assimilation (gross primary productivity, GPP, where GPP  $\leq 0$ , because  $CO_2$  uptake is denoted as a negative value) and ecosystem respiration (ER; a positive value) at half-hourly to decadal time scales, with the convention that fluxes into the ecosystem are negative (Wofsy and others 1993). Although we do not di-

rectly measure GPP and ER, NEE based on eddy covariance data can be partitioned into these counterparts to provide an approximation of ER and GPP and therefore a general understanding of the photosynthetic versus respiratory controls over NEE. This partitioning is calculated by employing the algorithm described in Reichstein and others (2005), using the ReddyProc software (Reichstein and others 2005; Papale and others 2006). The partitioning is performed based on nighttime temperature, where 'nighttime' is defined as PAR less than 50  $\mu$ mol m<sup>-2</sup> s<sup>-1</sup>. The algorithm fits a respiration model to the measured nighttime NEE data and then extrapolates the optimized model to the daytime using temperature observations during the day. An Arrhenius-type model after Lloyd and Taylor (1994) is used to derive and extrapolate the temperature dependence of ER:

$$ER = r_{b} \exp \left( E_{0} \left( \frac{1}{T_{ref} - T_{0}} - \frac{1}{T_{obs} - T_{0}} \right) \right)$$
 (1)

where  $r_{\rm b}$  (µmol C m<sup>-2</sup> s<sup>-1</sup>) is the base respiration at the reference air temperature  $T_{\rm ref}$  (°C), set to 15 (°C),  $E_0$  (°C) is the temperature sensitivity,  $T_{\rm obs}$  (°C) is the observed air temperature and parameter  $T_0$  (°C) is set to -46.02 °C as in Lloyd and Taylor (1994). A constant value for each year is derived for  $E_0$ , while  $r_{\rm b}$  is estimated every 5 days using a 15-days window. The difference between modeled ER and measured NEE provides the GPP estimate.

Bootstrapping was used to estimate the error (95% confidence interval) about the total NEE, GPP, and ER, and  $CH_4$ . The bootstrap calculated the confidence interval by: (1) constructing 2000 bootstrapped sample series by randomly sampling with replacement the observed total daily time series, (2) calculating an average from each constructed data series, and (3) calculating the grand mean ( $\pm$  95% CI) from the distribution of means calculated from the bootstrapped data series [Efron and Tibshirani 1998].

The  $CH_4$  data were converted to  $CO_2$  equivalents ( $CO_2$  e) by multiplying the  $CH_4$  flux by the 100-year global warming potential of methane, estimated at 28 (Myhre and others 2013).

We also calculated cumulative growing degree days (GDD) based on mean daily air temperature ( $T_a$ ) for both the measurement sites and the 30-year mean, as GDD =  $\Sigma$  max (2,  $T_i$  – 2), where  $T_i$  is the mean daily  $T_a$  and the base is 2 °C.

We evaluated the influence of the moisture status (Table 1) on fluxes by calculating adjusted means, including soil temperature ( $T_s$ , 7.5 cm

**Table 1.** Dates of Snow Return and Snow Melt and the Duration of Each Water Year (October 1–September 30) from October 1, 2004–September 30, 2018, from the Onset of the Seasonal Snowpack in the Fall to the Disappearance of the Snowpack in the Spring

Water year	Snow melt (month/day)	Snow return (month/day)		gth of snow son (days)	Total pro as snow	ecipitation (%)
2004–2005	10/20	4/28	190		36	
2005-2006	10/3	4/30	209		41	
2006-2007	9/27	4/15	200		18	
2007-2008	10/1	4/24	206		26	
2008-2009	9/30	4/27	209		51	
2009-2010	10/21	4/19	180		17	
2010-2011	10/11	4/23	194		42	
2011-2012	10/16	4/18	185		46	
2012-2013	10/14	5/21	219		55	
2013-2014	10/27	4/21	176		26	
2014-2015	10/3	4/19	198		24	
2015-2016	10/1	4/12	194		27	
2016-2017	10/20	4/28	190		48	
2017-2018	10/30	4/29	181		44	
Mean	10/12	4/25	195		36	
Mean rainfall (mm)	April-May	Jun	Jul	Aug	Sep-Oct	Total
	13	43	65	55	38	214

Also included is mean total rainfall by month from May to September, 2005–2018, based on the total rainfall depicted in Figure 1(a) and the percent of total precipitation as snow.

depth) for each of the fluxes NEE, ER, GPP and CH<sub>4</sub>:

Flux = Moisture Status 
$$\times$$
  $T_s$   
  $\times$   $(T_s \times Moisture Status) (2)$ 

The above analysis indicated that the slopes for the interaction term  $T_s \times \text{Moisture}$  Status were unequal (p < 0.0001) for all fluxes. We thus applied an unequal slopes model (Neter and others 1996) of the form:

$$Flux = Moisture Status \times (T_s \times Moisture Status)$$

(3)

For each of these analyses, we used the 'proc mixed' procedure in SAS (version 9.4, SAS Institute, Cary, NC).

We calculated total precipitation for each water year (October 1–September 30) from 2005 to 2018 based on rainfall and snow water equivalent data. We calculated the percent of snow water equivalent (SWE) of total precipitation for a given water year as:

Percent SWE = 
$$(Total SWE)/(Total SWE + Total Rain) \times 100$$

We determined the timing of snow return in the fall by observing at which point albedo remained above 0.3 in conjunction with mean daily air temperatures at or below freezing, and snow presence measured with the snow depth sensor and snow bucket. Timing of snow melt was determined by albedo measurements below 0.3, mean daily air temperatures above freezing, and an absence of snow measured by the snow depth sensor and the snow bucket. Our estimates were also cross-checked with visual webcam images.

We calculated the water budget (WB) for each growing season, May 15–October 15 as the difference between daily precipitation as rainfall (P<sub>daily</sub>; mm/day, and, occasionally, SWE in, for example, May 2013) and daily evapotranspiration (ET<sub>daily</sub>; mm/day, from eddy covariance measurements):

$$WB = P_{daily} - ET_{daily}$$
 (5)

ET includes both evapotranspiration from the plant canopy and evaporation from the moss and soil surface.

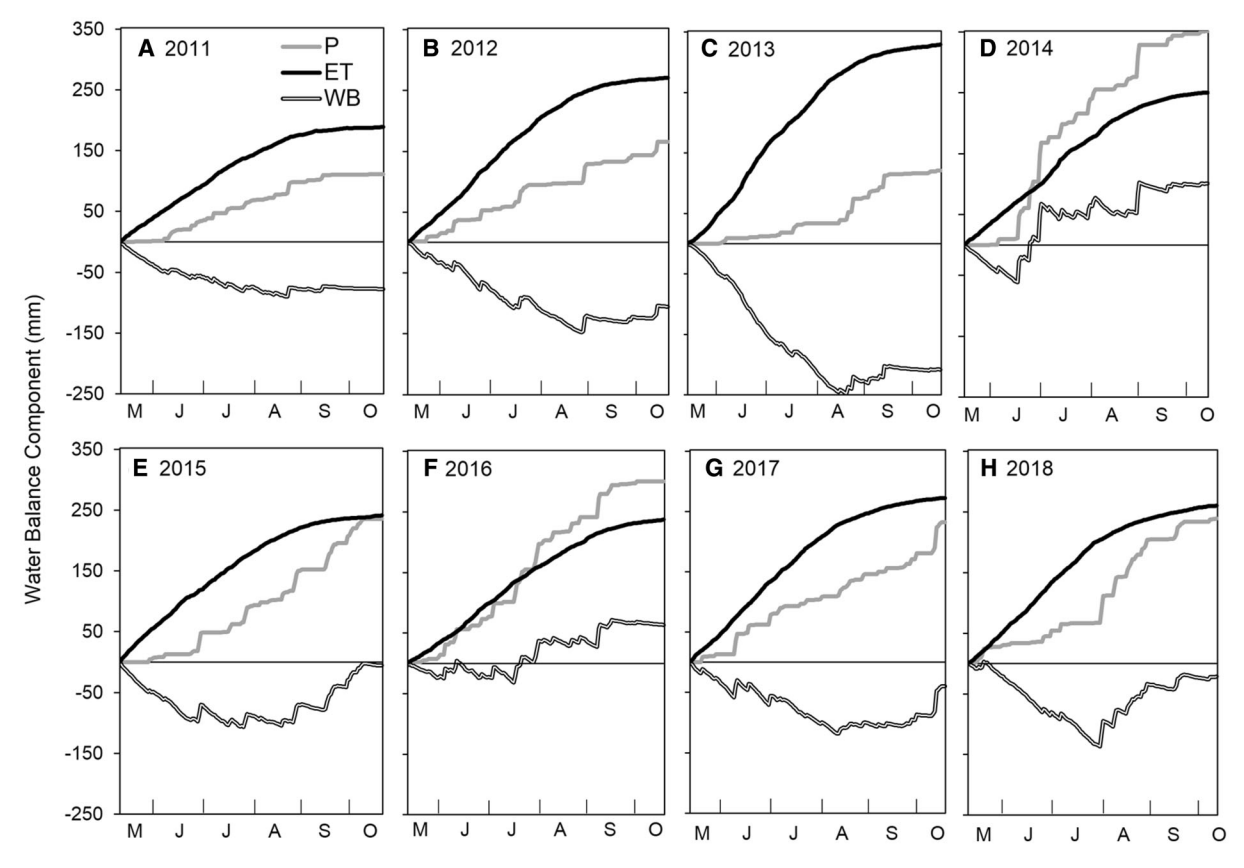


**Figure 2.** Cumulative precipitation as rainfall (P, mm d<sup>-1</sup>), evapotranspiration (ET, mm d<sup>-1</sup>), and water balance (WB = P – ET, mm d<sup>-1</sup>) from May 15 to October 15 for the years 2011–2018.

#### RESULTS

# Meteorology, Water Balance, and Ground Surface Conditions

From water years (defined as the 12-month period from October 1 to September 30) 2004–2018, the mean date of the return of the snowpack was

October 12 with disappearance by April 25. The mean length of the snow season is 195 days (Table 1). Precipitation as snow (mean of 116 mm each water year) accounted for a mean of 36% of the total precipitation as both rain (mean of 214 mm each water year) and snow (Figure 1A; Table 1). The greatest amounts of rain fell in July

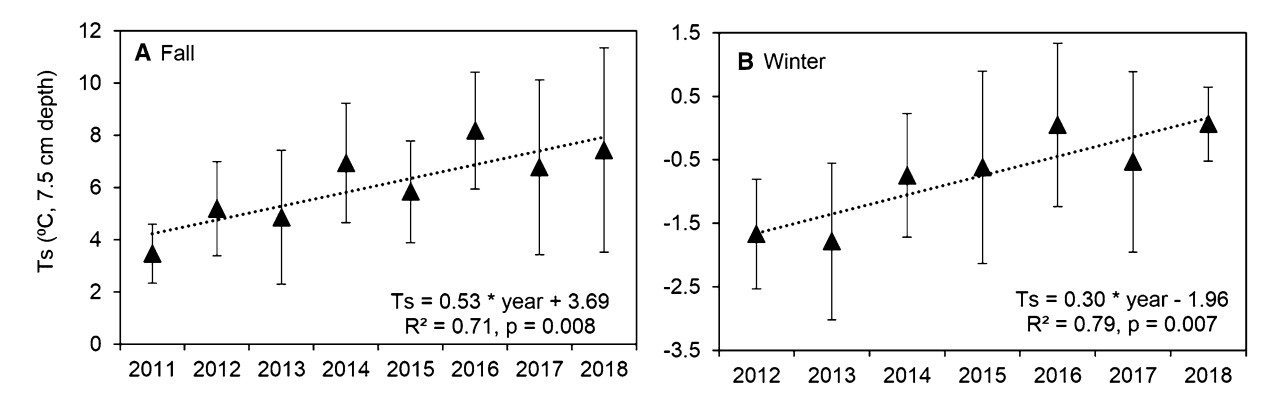


**Figure 3.** Trends in soil temperatures at 7.5 cm depth for (**a**) fall (September 1–October 14) and **b** winter (October 15–March 31). No significant trends were seen during spring (April 1–May 14) or summer (May 15–August 30). Because 'winter' refers to the period from October 15 to March 31, the given year also includes the period from October 15 to December 31 of the previous year.

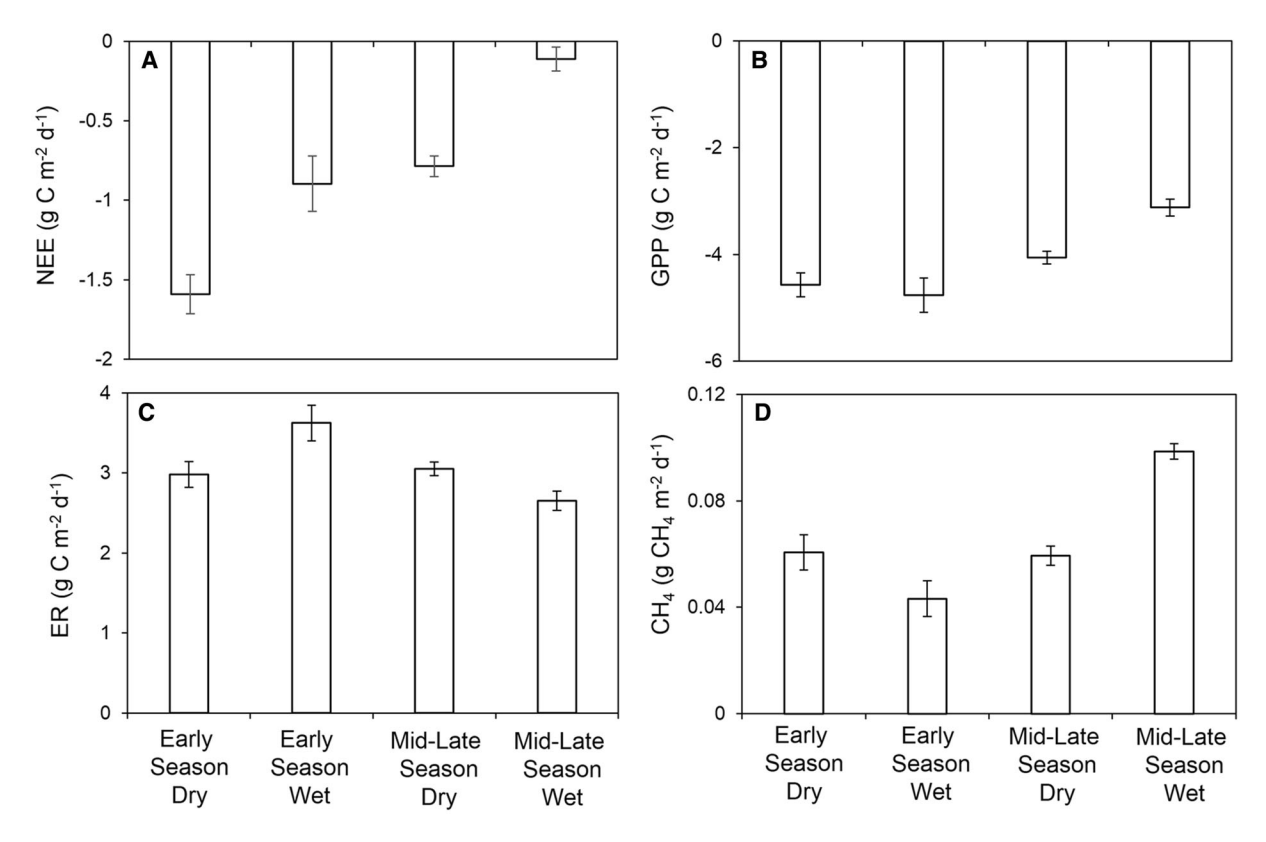


Figure 4. Least square means and standard errors as computed based on (Eq. 2) (see also Table 2). In **a–c** growing season NEE, GPP, and ER (g C m<sup> $^{-2}$ </sup> d<sup> $^{-1}$ </sup>; defined as May–September and **d** CH<sub>4</sub> emissions (g CH<sub>4</sub> m<sup> $^{-2}$ </sup> d<sup> $^{-1}$ </sup>) from 2011 to 2018 classified by the inundation status and season.

**Table 2.** Fixed Effects Models of Moisture/Inundation Status and Soil Temperature (Eq. 3) for NEE, ER, GPP (g C  $\text{m}^{-2}$  d<sup>-1</sup>) and CH<sub>4</sub> (g CH<sub>4</sub>  $\text{m}^{-2}$  d<sup>-1</sup>)

Modeled flux	Status	Equation
NEE	Inundated May–June*	$0.47 - 0.12 \times T_{\rm s}$
	Inundated July–Sept.*	$4.02 - 0.41 \times T_{\rm s}$
	Dry May–June*	$0.91 - 0.23 \times T_{\rm s}$
	Dry July–Sept.	$1.73 - 0.25 \times T_{\rm s}$
GPP	Inundated May–June	$-0.56-0.40 \times T_{s}$
	Inundated July–Sept.*	$2.11 - 0.53 \times T_{\rm s}$
	Dry May–June*	$-1.01 - 0.35 \times T_{\rm s}$
	Dry July–Sept.*	$0.66 - 0.46 \times T_{\rm s}$
ER	Inundated May–June*	$0.77 + 0.28 \times T_{\rm s}$
	Inundated July–Sept.*	$1.67 - 0.10 \times T_{\rm s}$
	Dry May–June*	$1.92 + 0.11 \times T_{\rm s}$
	Dry July–Sept.*	$1.44 - 0.16 \times T_{\rm s}$
CH <sub>4</sub>	Inundated May–June*	$0.01 + 0.004 \times T_s$
-	Inundated July–Sept.*	$-0.08 + 0.02 \times T_{\rm s}$
	Dry May–June*	$-0.04 + 0.04 \times T_{\rm s}$
	Dry July–Sept.*	$-0.03 + 0.01 \times T_{\rm s}$

 $T_s = soil$  temperature at 7.5 cm depth. A '\*' indicates the p value for a given intercept and slope are statistically significant at p < 0.05. The degrees of freedom for the models of NEE, ER and GPP are 1200 and that of CH<sub>4</sub> is 742.

and August each year, with April and May receiving the least (mean of 12 mm; Table 1). Most notably, 2014 was marked by the greatest total annual rainfall in the 100-year record for Fairbanks, AK (370 mm; Figure 1a; Alaska Climate Research Center, akclimate.org/Summary/Annual/Fairbanks/2014).

The water table remained above the surface during the growing season in 2008, 2013, 2014, 2017, and 2018 (Figure 1b). In 2013, snowmelt occurred nearly a month later (May 21) than the average (April 25), and even though the water table depth declined over a growing season marked by low rainfall (130 mm), it remained above the surface at the season's end. The record rainfall in 2014 flooded the fen in 2014 (Figure 1b). The second half of the 2016 growing season was flooded when amounts of rain fell during July. In 2017 and 2018, rainfall was high, but an above-average percent of precipitation as SWE (Table 1) also contributed to the inundated conditions.

The growing season water balance (P - ET) at the site showed a large amount of interannual vari-

ability, and could be either positive or negative in the flooded years (Figure 2). The water balance was most negative in 2013, with a cumulative value from May to October of -208 mm, with total ET of 329 mm and precipitation at 121 mm. The next year, in 2014, the water balance was the most positive, +100 mm, with precipitation of 350 mm and ET of 250 mm. In 2015, precipitation equaled ET (both at 238 mm), and the water balance was zero. The water balance in 2017 and 2018 was slightly negative (-47 mm in 2017 and -21 mmin 2018), yet the site exhibited flooded conditions similar to 2014 (Figure 1c). Over all the years, precipitation was more variable than ET, ranging from 110 to 350 mm for precipitation and from 187 to 329 mm for ET. This indicates that interannual variation in the water balance was driven more by variation in precipitation than by variation in ET.

Soil temperatures warmed from 2011 to 2018 in the winter and fall (Figure 3). There were no trends in the spring or summer soil temperatures, and there were also no trends seen in air temperatures

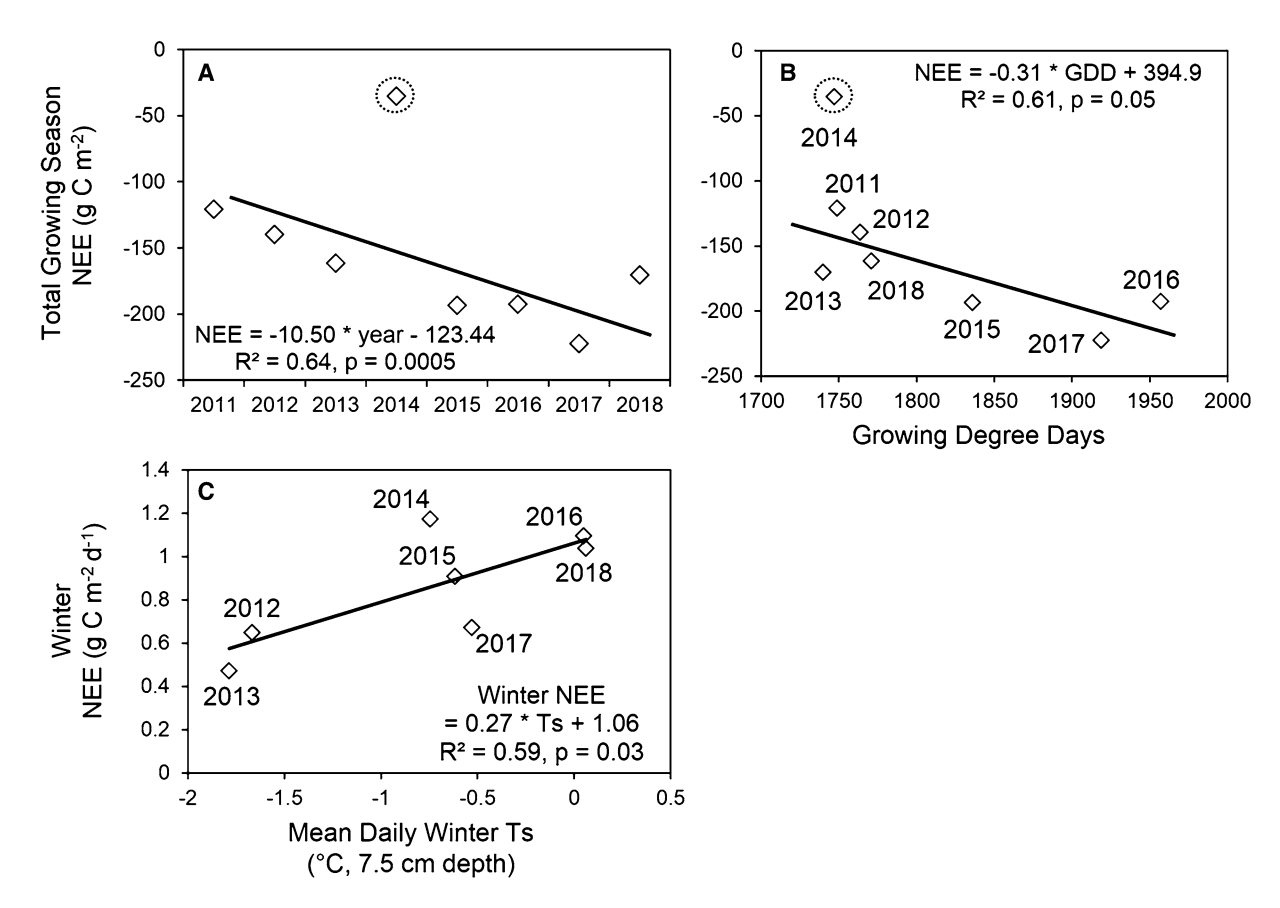
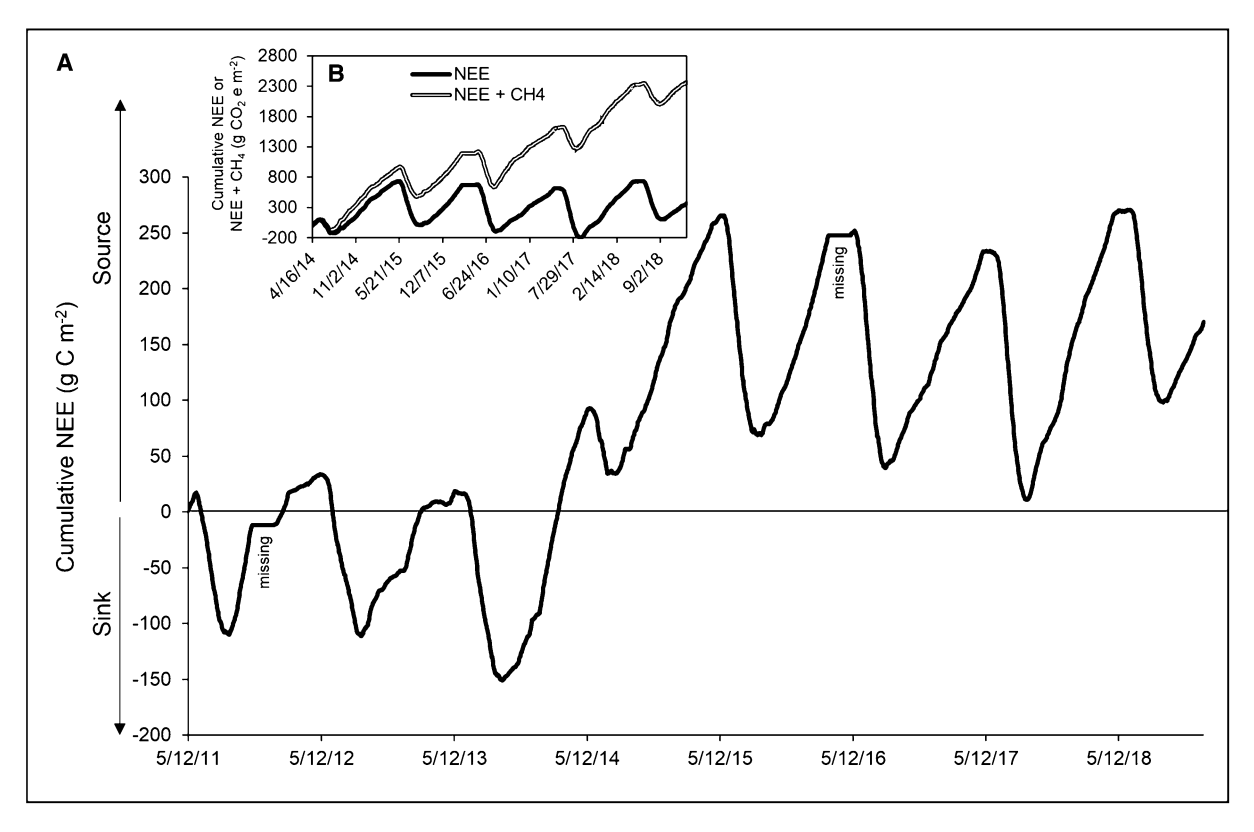


Figure 5. In **a**, total growing season NEE versus year and in **b** total growing season NEE versus growing degree days. In **a** and **b**, the regression line excludes the year 2014. In **c**, mean daily wintertime NEE versus mean daily wintertime soil temperature (with winter defined as in Figure 2 and only including days when data were available across all years).



**Figure 6.** In **a**, cumulative NEE (g C m<sup>-2</sup>, May 2011–December 2018, with missing data in 2011 and 2016 indicated by 'flat' areas on the graph). In **b**, cumulative NEE (g  $CO_2$  m<sup>-2</sup>) and cumulative NEE plus  $CH_4$  (g  $CO_2$  e m<sup>-2</sup>) from the beginning of  $CH_4$  measurements on April 17, 2014, to the end of  $CH_4$  collection on November 3, 2018.

in any season, indicating a decoupling of the soil and air temperatures.

#### Carbon Exchange

From May to September, CO<sub>2</sub> fluxes were generally related to inundation status and soil temperature (Figure 4; Table 2). NEE and GPP were least negative (for example, smallest amount of ecosystem C uptake;  $-0.1 \text{ g C m}^{-2} \text{ d}^{-1}$  for NEE and -3.1 gC m<sup>-2</sup> d<sup>-1</sup> for GPP; based on adjusted means controlling for soil temperature; Figure 4a, b) when the fen was inundated in the mid-late season, generally coincident with mid-late season rainfall. NEE was most negative (greatest ecosystem C uptake;  $-1.6 \text{ g C m}^{-2} \text{ d}^{-1}$ ) during early season dry periods (Figure 4a). ER was greatest during early season wet conditions (3.6 g C m<sup>-2</sup> d<sup>-1</sup>; Figure 4c).  $CH_4$  emissions (0.1 g  $CH_4$  m<sup>-2</sup> d<sup>-1</sup>) were 50% greater during mid-late season wet conditions compared to early season wet conditions (Figure 4d).

In addition to significant variations in growing season NEE due to inundation status, growing season NEE also showed a trend toward increased  $CO_2$  uptake (Figure 5a). This increase in growing season uptake was a strong linear trend by year  $(p=0.0005;\ R^2=0.64)$  if the anomalous year, 2014, was removed from the regression (Figure 5a), and was related to an increase in the cumulative growing degree days from May 16 to August 30, 2011–2017 (Figure 5b,  $p=0.05;\ R^2=0.61$ , again removing the year 2014 from the regression). Winter season NEE was related to soil temperatures, with warmer soil temperatures promoting release of  $CO_2$  (Figure 5d; p=0.03,  $R^2=0.59$ ).

Over the entire measurement period, the site was estimated as an overall source of  $CO_2$  from May 2011 to December 2018, of  $\sim 170 \pm 64$  g C m<sup>-2</sup>, although this estimate does not include data gaps in winter 2012 and 2016, when the data gaps were too long to be gap-filled ( $\sim 65$  days; Figure 6a). If the missing periods in winter were taken into account, this fen would be a larger source of  $CO_2$ . The year 2014 showed large emissions of  $CO_2$  because of large emissions of  $CO_2$  during the snow season (215  $\pm$  15 g C m<sup>-2</sup>; Figure 6), and ER was significantly greater during the growing season in 2014 (Figure 6). Converting the  $CH_4$  measurements to

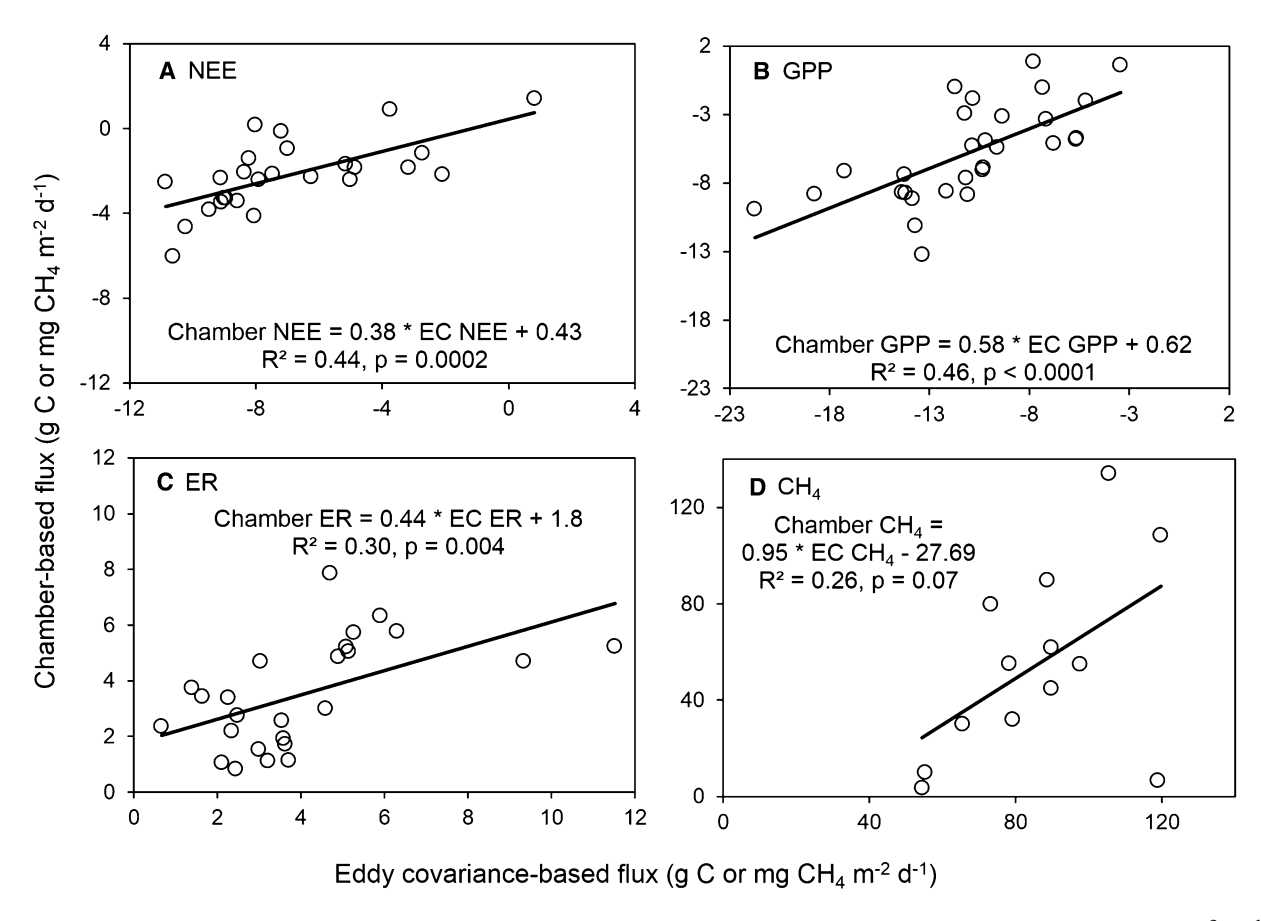


Figure 7. Eddy covariance-based measurements versus chamber-collected measurements of NEE, GPP, ER (g C m<sup>-2</sup> d<sup>-1</sup>), or CH<sub>4</sub> (mg CH<sub>4</sub> m<sup>-2</sup> d<sup>-1</sup>) for days during the growing season (June–August) in which both eddy covariance and chamber data were collected.

 $CO_2$  equivalents ( $CO_2$  e; Methods) and adding them to measured NEE resulted in increased emissions of 1997 g  $CO_2$  equivalents m<sup>-2</sup> (2345 g  $CO_2$  e m<sup>-2</sup> taking into account  $CH_4$  +  $CO_2$  versus 348 g  $CO_2$  e m<sup>-2</sup> taking only  $CO_2$  into account; Figure 6b).

# Eddy Covariance Versus Chamber Comparisons

Agreement between eddy covariance and chamber measurements was better for NEE ( $R^2 = 0.44$ , p = 0.0002; Figure 7a) and GPP ( $R^2 = 0.46$ , p < 0.0001; Figure 7b) than for ER ( $R^2 = 0.30$ , p = 0.004; Figure 7c). The eddy covariance data indicated greater uptake in terms of both NEE and GPP and greater release in ER than the chamber data. The relation between the eddy covariance and chamber data for CH<sub>4</sub> fluxes was weaker than for CO<sub>2</sub> fluxes ( $R^2 = 0.26$ , p = 0.07; Figure 7d).

### **DISCUSSION**

### Overview

Studies of the interannual variability of carbon and water fluxes in boreal fens are still relatively rare (Table 3). We know of no other studies that have examined these dynamics in response to the seasonality of dry periods versus inundated periods in these ecosystems. Here, we examined the interannual variability in carbon and water fluxes at a rich fen in interior Alaska that has experienced early season inundation following snowmelt and late season inundation in conjunction with periods of rain. There were also periods when the fen was dry, with a water table depth below the surface. The NEE summed from May 2011 to December 2018 indicated the site was a source of CO<sub>2</sub>, with a shift from net annual sink to net annual source occurring in 2014 (Figure 6a). The inclusion of methane emissions showed that the fen is an even greater source of carbon emissions (Figure 6b).

Published Estimates of Mean (Standard Deviation) Annual Net Ecosystem Exchange (NEE), Gross Primary Productivity (GPP) and Ecosystem Respiration (ER), and  $CH_4$  Emissions (g C m<sup>-2</sup> y<sup>-1</sup>  $\pm$  Standard Deviation) in Boreal Fens at Sites with Eddy Covariance Measurements Taken Over Multiple Years for the Full Annual Cycle

Site description	Lat./long.	Years	NEE	GPP	ER	$\mathrm{CH}_4$	CH <sub>4</sub> Reference
Rich fen, northern Finland	67°59′ N, 24°12′ E	2006–2008	<i>-</i> 31 ± 39	$-390 \pm 13$	$-390 \pm 13 - 353 \pm 20$	1	Aurela and others (2009)
Mesotrophic fen, northern Finland	69°08′ N, 27°17′ E	1997–2002	$-22 \pm 20$	1	ı	1	Aurela and others (2004)
Poor fen, southern Finland	61°50′ N, 24°12′ E	$2005-2013^a$	$-58 \pm 41$	$-379 \pm 79 321 \pm 41$	$321 \pm 41$	$10 \pm 2$	Rinne and others (2018)
Minerotrophic fen, northern Sweden,	68°20′ N, 19°03′ E	2012-2013	$-66 \pm 11$	ı	1	$21 \pm 1$	$21 \pm 1$ Jammet and others (2017)
Moderately rich treed fen, Alberta, Canada	54°95′ N, 112°46′ W	2004-2009	$-189 \pm 47$	ı	I	1	Flanagan and Syed (2011)
Poor sedge fen, northern Sweden	64°11′ N, 19°33′ E	2001–2012	$-58 \pm 21$	$-336 \pm 98  278 \pm 92$	$278 \pm 92$	1	Peichl and others (2014)
Rich Fen, Interior Alaska	64.70° N, 148.32° W	2012-2017 <sup>b</sup>	$36 \pm 130$	$-480 \pm 67$	$-516 \pm 88$	1	This study
Overall mean			$-55 \pm 68$	$-396 \pm 64$	$367 \pm 60$	$16 \pm 2$	

A negative value indicates a sink of C, and a positive value is a source to the atmosphere

 $^{4}$ Excludes 2009 due to loss of data.  $^{5}$ Excludes 2016 due to loss of data.

In our discussion as follows, we consider the timing of inundation and dry periods, and how these related to the interannual carbon dynamics. We evaluate our eddy covariance—chamber comparisons in the context of this site and other studies that have made similar comparisons.

# CO<sub>2</sub> Dynamics

Our results suggest that the mechanism of inundation largely controls C balance. Mean daily NEE at the fen varied depending on the inundation conditions at the site, with the least amount of CO<sub>2</sub> taken up when the fen was inundated late in the season in conjunction with mid-late season rainfall, as occurred in 2014 and late 2016 (Table 1; Figures 2d, f, 4a). The optimal conditions for net uptake occurred during early season dry conditions (Figure 4a). GPP showed less variability across early season dry, early season wet, and mid-late season dry periods, but did show reduced uptake during mid-late season wet (Figure 4b). ER was also slightly suppressed during mid-late season wet conditions (Figure 4c). Thus, this slight suppression of both GPP and ER in mid-late season wet conditions contributed to reduced net C uptake.

We inferred the source of inundation in this fen from runoff and snowmelt early in the growing season and from rainfall in the mid-late growing season based on the timing of the snowmelt and seasonal rainfall patterns. Our understanding of the seasonality of the groundwater delivery in this fen is still limited, although it likely flows out southward toward the nearby Tanana River. The topography northward of the fen gently slopes toward it such that these surrounding permafrost forests may act as source of water draining toward the fen. The concentrations of base cations measured within the peat pore water loosely tracked those measured in the Tanana, suggesting some degree of runoff connectivity via off-site upwelling and lateral transport (Racine and Walters 1994; Kane and others 2010). Although any dissolved organic C in runoff would also represent even more losses of C from this system when flooding permits high connectivity, these exports are likely to be small compared with gaseous emissions (in the order of 4.5–12.0 g C m<sup>-2</sup> year<sup>-1</sup>, for example, Kane and others 2006). To more fully address how the source of inundation in this fen influences total carbon fluxes, including gaseous and lateral losses, additional information on the runoff from the surrounding higher elevation landscape and on groundwater flow is necessary.

In comparing published interannual eddy covariance measurements of boreal fen NEE, the fen in this study is the only fen that is estimated as a mean source of CO2 across measurement years (Table 3). These studies showed less variability in the water table depth over the growing season than we found, and typically, the reported water table depth was below the surface, with some sites experiencing longer-term drying trends example, Flanagan and Syed 2011). This is notable in the context of our site which remained inundated in 2014, 2017, and 2018. Peichl and others (2014) reported substantially less net CO<sub>2</sub> uptake in a year with an exceptionally strong late summer drop in the water table. These studies also did not document a significant winter warming, as we have here. This helps to emphasize the importance of 2014 when CO2 emissions were anomalously high during winter (Figure 5c, 6a) and NEE was near zero during the 2014 growing season with record rainfall (Figure 5a). Consequently, the site would have been nearly neutral or a slight source if not for 2014, illustrating the long-term influence of one extreme year. Therefore, the trend in greater summer uptake of CO2 with an increase in GDDs indicates the fen appears resilient to these drastic swings in the water table in terms of NEE (Figure 5a), unless inundated later in the season, as occurred in 2014 with the extreme rainfall. If years with extreme rainfall occur more frequently, particularly in conjunction with warming winter soil temperatures (Figures 3, 5c), we may expect a reduction in boreal fen CO<sub>2</sub> uptake.

#### CH<sub>4</sub> Dynamics

Flooding during the early season was related to lowered CH<sub>4</sub> emissions, while flooding later in the season was related to increased CH<sub>4</sub> emissions. In fens and other wetlands, CH4 is produced under anaerobic conditions by methanogenic bacteria, whereas CH<sub>4</sub> consumption occurs through oxidizing micro-organisms in the aerobic peat layers. Previous research has found that a high water table results in increases in CH4 emissions, in a balance between anaerobic CH<sub>4</sub> production below the water table and oxidation above it (Bridgham and others 2013; Olefeldt and others 2017). However, recent studies of interannual CH4 eddy covariance measurements in a temperate fen (Pugh and others 2017) and boreal fen (Rinne and others 2018) found little relation between water table position and CH<sub>4</sub> fluxes, with two possible explanations. First, a high water table may lower CH<sub>4</sub> emissions due to the complete submersion of

aerenchymatous plants. Alternatively, an increase in the relative activities of aerenchymatous plants during flooding (McPartland and others 2019) could actually have an oxidizing effect within the peat (Strack and others 2017; Rupp and others 2019). Second, if a high water table is due to rainfall (as in 2014 in the present study), this has a significant oxidizing effect on pore water redox potential (Mitchell and Branfireun 2005). Not only can this suppress methanogenesis, but this vertical stratification of water with low dissolved CH4 concentrations occurring above higher CH<sub>4</sub> concentrations can slow diffusion through the peat during saturated conditions, as the diffusion through water is slower than through air-filled pore space (Rinne and others 2018). Moreover, surface water would be much more oxidized with meteoric inputs—which would likely result in CH<sub>4</sub> oxidation, similar to the observed changes in redox species after heavy rainfall in peatland catchments of Northwest Ontario (Mitchell and Branfireun 2005). The magnitude of this oxidizing effect has been shown to increase with the duration (Mitchell and Branfireun 2005) and frequency (Radu and Duval 2018) of rainfall events. Our present study agrees with these studies finding no relation between CH<sub>4</sub> emissions and water table depth: with higher CH<sub>4</sub> emissions under inundation with midlate season rainfall, but lower emissions when inundation under inundated conditions following snowmelt (Figure 4d).

# Eddy Covariance Versus Chamber Measurements

Manual chamber measurements are an effective technique to study plot-scale experimental manipulations. The eddy covariance technique provides continuous measurements, but requires large homogeneous areas. The fen footprint of the eddy covariance measurements is a homogeneous area of grasses, sedges, and forbs, and lies outside the experimental manipulation (Euskirchen and others 2014).

In a comparison of eddy covariance versus chamber measurements in forests across the globe, Wang and others (2017) found that eddy covariance measurements overestimated NEE by 25%, and underestimated ER by 10% and GPP by 3%. The overestimation of NEE was greatest in sites with complex topography and at sites with openpath eddy covariance systems that are marked by a surface-heating effect. Furthermore, eddy covariance only directly measures NEE, and as such, the GPP and ER estimates derived from the NEE may

introduce error (Lasslop and others 2012). Statistical theory has shown that typically 10-20 chambers are needed to sample a representative portion of the canopy and its natural variability (Steel and Torrie 1960). However, it is more challenging to find agreement between CH4 chamber and eddy covariance measurements because emissions may show more spatial variability than CO2 fluxes. In this case, factors affecting reduction-oxidation potential that can occur on relatively small spatial scales, such as fluctuations in the water table position near the peat surface or presence of aerenchymatous plants (Agethen and others 2018), are likely to introduce variability in CH4 fluxes measured at the chamber scale, whereas deeper redox processes are better reflected on the spatial scale on which the eddy covariance measurements were made.

#### CONCLUSION

Although boreal fens are typically considered sinks of CO<sub>2</sub> (Table 3), the rich fen in this study acted as a source of  $CO_2$  of  $170 \pm 64$  g C m<sup>-2</sup> from 2011 to 2018. This source strength was largely related to both warming winter soil temperatures which increased winter CO2 emissions, and mid-late season inundation, which decreased GPP and reduced net C uptake. Methane emissions were at their lowest during early season inundation and largest in midlate season inundation. Wetland biogeochemical models have extensively incorporated dynamics related to hydrology and temperature into modeling CO2 and CH4 (Fan and others 2013; Wu and Roulet 2014; Li and others 2016), but our study suggests that additional dynamics should be considered. This includes the mechanism and timing of inundation, especially extreme rain events because they can have a long-term impact and may become more prevalent in the future. Furthermore, these models should consider the source of boreal fen inundation in a given year, including precipitation, runoff and groundwater flow, because the mechanism of inundation affects CO<sub>2</sub> and CH<sub>4</sub> emissions. Remotely sensed datasets of wetlands in boreal regions (for example, Clewley and others 2015), and of water table position (for example, Bechtold and others 2018), should also consider interannual variations due to differences in precipitation inputs, runoff, and groundwater flow. Thus, to understand the resiliency of the carbon sink strength of these fens to changes in climate and extreme precipitation events, it is important to consider the timing and source of inundation: precipitation inputs from

rain versus runoff from snow and groundwater flow.

#### ACKNOWLEDGEMENTS

This project was funded by National Science Foundation Grants DEB LTREB 1354370, DEB-0425328, DEB-0724514, and DEB-0830997. Bonanza Creek Long Term Experimental Research station provided lab space, equipment, and time to this project. This research was also funded by the US Geological Survey and received in-kind support from the US Forest Service Northern Research Station.

#### DATA AVAILABILITY

The data are available through the Bonanza Creek Long Term Ecological Research Site data portal: https://www.lter.uaf.edu/data/data-catalog.

#### REFERENCES

- Agethen S, Sander M, Waldemer C, Knorr K-H. 2018. Plant rhizosphere oxidation reduces methane production and emission in rewetted peatlands. Soil Biology and Biochemistry 125:125–35.
- Aurela M, Laurila T, Tuovinen J-P. 2004. The timing of snow melt controls the annual CO<sub>2</sub> balance in a subarctic fen. Geophysical Research Letters 31:L16119. https://doi.org/10.1029/2004GL020315
- Aurela M, Lohila A, Tuovienn J-P, Hatakka J, Riutta T, Laurila T. 2009. Carbon dioxide exchange on a northern boreal fen. Boreal Environment Research 14:699–710.
- Bechtold M, Schlaffer S, Tiemeyer B, De Lannoy G. 2018. Inferring Water Table Depth Dynamics from ENVISAT-ASAR C-Band Backscatter over a Range of Peatlands from Deeply-Drained to Natural Conditions. Remote Sensing 10:536. https://doi.org/10.3390/rs10040536.
- Bridgham SD, Cadillo-Quiroz H, Keller JK, Zhaung Q. 2013. Methane emissions from wetlands: biogeochemical, microbial, and modeling perspectives from local to global scales. Global Change Biology 19:1325–46.
- Chivers MR, Turetsky MR, Waddington JM, Harden JW, McGuire AD. 2009. Effects of experimental water table and temperature manipulations on ecosystem CO<sub>2</sub> fluxes in an Alaskan rich fen. Ecosystems 12:1329–42.
- Churchill AC, Turetsky MR, McGuire AD, Hollingsworth TN. 2015. Response of plant community structure and primary productivity to experimental drought and flooding in an Alaskan fen. Canadian Journal of Forest Research. 45:185–93. https://doi.org/10.1139/cjfr-2014-0100.
- Clewley D, Whitcomb J, Moghaddam M, McDonald K, Chapman B, Bunting P. 2015. Evaluation of ALOS PALSAR Data for High-Resolution Mapping of Vegetated Wetlands in Alaska. Remote Sensing 7:7272–97. https://doi.org/10.3390/rs70607272.
- Efron B, Tibshirani R. 1998. *An Introduction to the Bootstrap*. Boca Raton: Chapman and Hall.
- Euskirchen ES, Edgar C, Turetsky MR, Waldrop MP, Harden JW. 2014. Differential response of carbon fluxes to climate in three

- peatland ecosystems that vary in the presence and stability of permafrost. Journal of Geophysical Research: Biogeosciences 119:1576–95. https://doi.org/10.1002/2014JG002683.
- Euskirchen ES, Bennett A, Breen AL, Genet H, Lindgren M, Kurkowski T, Mcuire AD, Rupp TS. 2016. Consequences of changes in vegetation and snow cover for climate feedbacks in Alaska and northwest Canada. Environmental Research Letters 11:105003. https://doi.org/10.1088/1748-9326/11/10/105003.
- Euskirchen ES, Bret-Harte MS, Shaver GR, Edgar CW, Romanovsky VE. 2017. Long-term release of carbon dioxide from arctic tundra ecosystems in northern Alaska. Ecosystems 20:960–74. https://doi.org/10.1007/s10021-016-0085-9.
- Falge E et al. 2001. Gap filling strategies for defensible annual sums of net ecosystem exchange. Agricultural and Forest Meteorology 107:43–69.
- Fan Z, McGuire AD, Turetsky MR, Harden JW, Waddington JM, Kane ES. 2013. The response of soil organic carbon of a rich fen peatland in interior Alaska to projected climate change. Global Change Biology 19:604–20.
- Flanagan LB, Syed KH. 2011. Simulation of both photosynthesis and respiration in response to warmer and drier conditions in a boreal peatland ecosystem. Global Change Biology 17:2271–87.
- Helbig M, Wischnewsi K, Natascha K, Chasmer LE, Quinton WL, Detto M, Sonnentag O. 2016. Regional atmospheric cooling and wetting effect of permafrost thaw-induced boreal forest loss. Global Change Biology 22:4048–66.
- Jammet M, Dengel S, Kettner E, Parmentier F-J, Wik M, Crill P, Friborg T. 2017. Year-round CH<sub>4</sub> and CO<sub>2</sub> flux dynamics in two contrasting freshwater ecosystems of the subarctic. Biogeosciences 14:5189–216. https://doi.org/10.5194/bg-14-5189-2017.
- Jorgenson MT, Racine CH, Walters JC, Osterkamp TE. 2001. Permafrost degradation and ecological changes associated with a warming climate in central Alaska. Climatic Change 48:551–79.
- Jorgenson MT, Osterkamp TE. 2005. Response of boreal ecosystems to varying modes of permafrost degradation. Canadian Journal of Forest Research 35:2100–11.
- Kane ES, Valentine DW, Michaelson GJ, Fox JD, Ping C-L. 2006. Controls over pathways of carbon efflux from soils along climate and stand productivity gradients in interior Alaska. Soil Biology and Biochemistry. 38:1438–50.
- Kane ES, Turetsky MR, Harden JW, McGuire AD, Waddington JM. 2010. Seasonal ice and hydrological controls on dissolved organic carbon and nitrogen concentrations in a boreal-rich fen. Journal of Geophysical Research 115:G04012. https://doi.org/10.1029/2010JG001366.
- Kolka R, Trettin C, Tang W, Krauss K, Bansal S, Drexler J, Wickland K, Chimner R, Hogan D, Pindilli EJ, Benscoter B, Tangen B, Kane E, Bridgham S, and Richardson C. 2018. Chapter 13: Terrestrial wetlands. In *Second State of the Carbon Cycle Report (SOCCR2): A Sustained Assessment Report* [Cavallaro N, Shrestha G, Birdsey R, Mayes MA, Najjar RG, Reed SC, Romero-Lankao P, and Zhu Z (eds.)]. U.S. Global Change Research Program, Washington, DC, USA, pp. 507-567, https://doi.org/10.7930/SOCCR2.2018.Ch13.
- Lara MJ, Genet H, McGuire AD, Euskirchen ES, Zhang Y, Brown D, Jorgenson MT, Romanovsky V, Breen A, Bolton WR. 2016. Thermokarst rates intensify due to climate change and forest fragmentation in an Alaskan boreal forest lowland. Global

- Change Biology 22:816–29. https://doi.org/10.1111/gcb.1312
- Laine AM, Mäkiranta P, Laiho R, Mehtätalo L, Penttilä T, Korrensalo A, Minkkinen K, Fritze H, Tuittila E-S. 2019. Warming impacts on boreal fen CO 2 exchange under wet and dry conditions. Global Change Biology 25:1995–2008.
- Lasslop G, Migliavacca M, Bohrer G, Reichstein M, Bahn M, Ibrom A, Jacobs C, Kolari P, Papale D, Vesala T, Wohlfahrt G, Cescatti A. 2012. On the choice of the driving temperature for eddy-covariance carbon dioxide flux partitioning. Biogeosciences 9:5243–59.
- Lehmann J, Coumou D. 2015. The influence of mid-latitude storm tracks on hot, cold, dry and wet extremes. Scientific Reports 5: art. No. 17491, https://doi.org/10.1038/srep17491
- Li T, Raivonen M, Alekseychik P, Aurela M, Lohila A, Zheng X, Zhang Q, Wang G, Mammarella I, Rinne J, Yu L, Xie B, Vesala T, Zhang W. 2016. Importance of vegetation classes in modeling CH4 emissions from boreal and subarctic wetlands in Finland. Science of the Total Environment 572:1111–22.
- Lloyd J, Taylor JA. 1994. On the Temperature Dependence of Soil Respiration. Functional Ecology 8:315–23.
- Massman WJ. 2000. A simple method for estimating frequency response corrections for eddy covariance systems. Agricultural and Forest Meteorology 104:185–98.
- Massman WJ. 2001. Reply to comment by Rannik on "A simple method for estimating frequency response corrections for eddy covariance systems". Agricultural and Forest Meteorology 107:247–51.
- McPartland MY, Kane ES, Falkowski MJ, Kolka R, Turetsky MR, Palik B, Montgomery RA. 2019. The response of boreal peatland community composition and NDVI to hydrologic change, warming, and elevated carbon dioxide. Global Change Biology 25:93–107.
- Mitchell CPJ, Branfireun BA. 2005. Hydrogeomorphic Controls on Reduction-Oxidation Conditions across Boreal Upland-Peatland Interfaces. Ecosystems 8:731–47.
- Neter J, Kutner MH, Nachtsheim CJ, Wasserman W. 1996. Applied Linear Statistical Models. 4th edn. Boston, MA: McGraw-Hill.
- Olefeldt D, Euskirchen ES, Harden J, Kane E, McGuire AD, Waldrop M, Turetsky MR. 2017. Greenhouse gas fluxes and their cumulative response to inter-annual variability and experimental manipulation of the water table position in a boreal fen. Global Change Biology 23:2428–40.
- Papale D et al. 2006. Towards a standardized processing of net ecosystem exchange measured with eddy covariance technique: Algorithms and uncertainty estimation. Biogeosciences 3:571–83.
- Peichl M, Oquist M, Lofvenius MO, Ilstedt U, Sagerfors J, Grelle A, Lindroth A, Nilsson MB. 2014. A 12-year record reveals pre-growing season temperature and water table level threshold effects on the net carbon dioxide exchange in a boreal fen. Environmental Research Letters. 9(5). https://doi.org/10.1088/1748-9326/9/5/055006
- Racine CH, Walter JC. 1994. Groundwater-Discharge Fens in the Tanana Lowlands. Interior Alaska. Arctic and Alpine Research. 26:418–26.
- Radu DD, Duval TP. 2018. Impact of rainfall regime on methane flux from a cool temperate fen depends on vegetation cover. Ecological Engineering 114: 76 -87. https://doi.org/10.1016/j.ecoleng.2017.06.047

- Reichstein M et al. 2005. On the separation of net ecosystem exchange into assimilation and ecosystem respiration: Review and improved algorithm. Global Change Biology 11:1424–39.
- Rinne J, Tuittila E-S, Peltola O, Li X, Raivonen M, Alekseychik P et al. 2018. Temporal variation of ecosystem scale methane emission from a boreal fen in relation to temperature, water table position, and carbon dioxide fluxes. Global Biogeochemical Cycles 32:1087–106. https://doi.org/10.1029/2017G B005747.
- Rupp DR, Kane ES, Dieleman C, Keller JK, Turetsky MR. 2019. Plant functional group effects on peat carbon cycling in a boreal rich fen. Biogeochemistry. 144:305–27. https://doi.org/10.1007/s10533-019-00590-5.
- Sonnentag O, van der Kamp G, Barr AG, Chen JM. 2010. On the relationship between water table depth and water vapor and carbon dioxide fluxes in a minerotrophic fen. Global Change Biology 16:1762–76. https://doi.org/10.1111/j.1365-2486.20 09.02032.x.
- Steel RGD, Torrie JH. 1960. *Principles and Procedures of Statistics with Special Reference to the Biological Sciences*. New York: McGraw Hill. pp 187–287.
- Strack M, Mwakanyamale K, Fard GH, Bird M, Berube V, Rochefort L. 2017. Effect of plant functional type on methane dynamics in a restored minerotrophic peatland. Plant and Soil 410:231–46.
- Sulman BN, Desai AR, Saliendra NZ, Lafleur PM, Flanagan LB, Sonnentag O, Mackay DS, Barr AG, van der Kamp G. 2010. CO<sub>2</sub> fluxes at northern fens and bogs have opposite responses to inter-annual fluctuations in water table. Geophysical Research Letters 37:L19702. https://doi.org/10.1029/2010G L044018.
- Tebaldi C, Hayhoe K, Armblaster JM, Meehl GA. 2006. Going to the extremes: An intercomparison of model-simulated historical and future changes in extreme events. Climatic Change 79:185–211.

- Turetsky MR, Treat CC, Waldrop MP, Waddington JM, Harden JW, McGuire AD. 2008. Short-term response of methane fluxes and methanogen activity to water table and soil warming manipulations in an Alaskan peatland. Journal of Geophysical Research 113, G00A10, https://doi.org/10.1029/2007jg000496.
- Van Cleve K, Chapin FS III, Ruess RW. 2018. Bonanza Creek LTER: Hourly Precipitation Weighing Bucket Measurements from 1988 to Present in the Bonanza Creek Experimental Forest near Fairbanks, Alaska, Bonanza Creek LTER University of Alaska Fairbanks. BNZ:183,http://www.lter.uaf.edu/data/data-detail/id/183. https://doi.org/10.6073/pasta/1620b43e9ad1755b5d2001537aa13ad5
- Vitt DH, Halsey LA, Bauer IE, Campbell C. 2000. Spatial and temporal trends of carbon sequestration in peatlands of continental western Canada through the Holocene. Canadian Journal of Earth Science 37:683–93.
- Wang X, Wang C, Bond-Lamberty B. 2017. Quantifying and reducing the differences in forest CO2-fluxes estimated by eddy covariance, biometric and chamber methods: A global synthesis. Agricultural and Forest Meteorology. 247:93–103.
- Webster KL, Bhatti JS, Thomson DK, Nelson SA, Shaw CH, Bona KA, Hayne SL, Kurz WA. 2018. Spatially-integrated estimates of net ecosystem exchange and methane fluxes from Canadian peatlands. Carbon Balance and Management 13:16. h ttps://doi.org/10.1186/s13021-018-0105-5.
- Wofsy SC, Goulden ML, Munger JW, Fan SM, Bakwin PS, Daube BC, Bassow SL, Bazzaz FA. 1993. Net exchange of CO2 in a midlatitude forest. Science 260:1314–17.
- Wu J, Roulet NT. 2014. Climate change reduces the capacity of northern peatlands to absorb the atmospheric carbon dioxide: The different responses of bogs and fens. Global Biogeochemical Cycles 27:1005–24.
- Yu ZC. 2012. Northern peatland carbon stocks and dynamics: a review. Biogeosciences 9:4071–85.